ROYAL SOCIETY OF CHEMISTRY

PAPER

Check for updates

Tracking and recording of intracellular oxygen concentration changes in cell organelles: preparation and function of azide-modified fluorescent probes†

Hiroki Makanai, Miei Kanda, Sae Harada, Tatsuya Nishihara [ID] and Kazuhito Tanabe [ID]*

Tracking hypoxic environments and changes in oxygen levels contribute to the elucidation of pathological mechanisms. In this study, we attempted to design molecular probes that can be activated to show fluorescence under hypoxic conditions and that can move to specific cell organelles. Considering that azide groups were selectively reduced to primary amines by reductases under hypoxic conditions, we prepared Hoechst and fluorophore Cy-5 derivatives with azide groups (Hoechst-N_3 and Cy-N_3) as hypoxia probes. Hoechst-N_3 and Cy-N_3 showed weak fluorescence, but once activated in the cytosol of hypoxic cells, they exhibited robust fluorescence and then moved to their target organelles, the cell nucleus and mitochondria. In addition, when these probes were administered to the cells in the proper sequence, each probe was activated in response to the intracellular oxygen concentration at that point and exhibited oxygen concentration-dependent fluorescence at the target organelle. By measuring the fluorescence intensity of the cell nucleus and mitochondria, we successfully traced the history of changes in intracellular oxygen levels. Thus, we achieved tracking and recording of oxygen status in the cells.

Introduction

Oxygen molecules are functional substances that actively work in living systems. Fluctuation of oxygen levels in cells significantly affects their functions such as cell growth, differentiation, and signaling.[1–3] One of the most important behaviors of molecular oxygen in cells is that fluctuations in its levels can profoundly affect resistance to therapy, especially radiotherapy for cancer.[4–6] Tumor hypoxia is closely associated with the malignant phenotype of cancer cells, resistance to cancer radiotherapies, and a high mortality rate among patients with cancer.[7–9] Therefore, tracking the oxygen status has been imperative to understand the cellular functions and provide appropriate medical treatment.

Organelle-targeted fluorescent probes have been designed to visualize cellular chemical messengers and functions with a high degree of accuracy, making them valuable tools for studying biochemical reactions and events in each

organelle.[10–16] Several probes have been designed to monitor oxygen status in specific organelles. For example, Tobita and coworkers reported mitochondria-targeted phosphorescent probes bearing cationic iridium complexes.[11] Our group prepared cell nucleus-targeted phosphorescent probes using the Hoechst molecule and ruthenium complexes.[15] These conventional probes interact directly with oxygen molecules and exhibit oxygen-responsive phosphorescence, and they could detect the real-time oxygen status in cells. However, emission intensity of these probes changed instantly when oxygen concentration changes, and thus, they could not detect the history of changes in intracellular oxygen levels in spite that functional behavior of tumor cells as well as the cope with therapeutic insults, differ depending upon the extent and history of the oxygen variation.[17]

Herein, we newly designed fluorescent probes, which were selectively activated by reductases in hypoxic cells (Fig. 1), to show the history of changes in intracellular oxygen levels. After their activation in cytosol of hypoxic cells, the probes were transported to their target organelles. Thus, these probes accumulated in their target organelles while retaining information on intracellular oxygen levels. Given that the azide groups were reduced to primary amines by reduction enzymes in hypoxic cells[18,19] and often quenched fluorescence emission,[20] we designed a derivative of the nuclear-staining reagent

Department of Chemistry and Biological Science, College of Science and Engineering, Aoyama Gakuin University, 5-10-1 Fuchinobe, Chuo-ku, Sagamihara, 252-5258, Japan. E-mail: tanabe.kazuhito@chem.aoyama.ac.jp
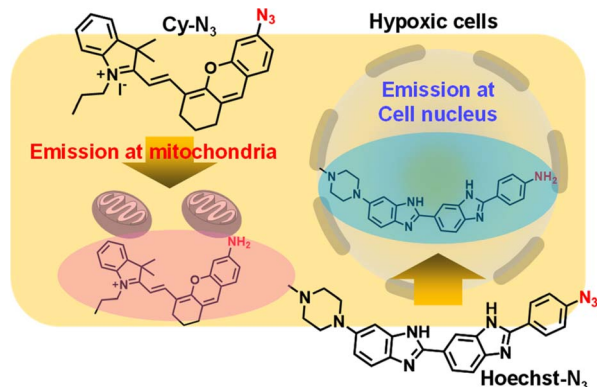
Fig. 1 Illustration of hypoxia probes that were accumulated in cell nucleus (Hoechst-N$_3$) and mitochondria (Cy-N$_3$).

Fig. 2 Fluorescence spectra of Hoechst-N$_3$ (A–C) and Cy-N$_3$ (D–F) after enzymatic reduction: Hoechst-N$_3$ (500 nM) or Cy-N$_3$ (500 nM) were incubated with rat liver microsome (1.0 mg mL^{-1}) at 37 °C in phosphate buffer (pH 7.4) and then the fluorescence spectra were measured. Excitation wavelength was 405 and 685 nm for Hoechst-N$_3$ and Cy-N$_3$, respectively. (A and B) Emission of Hoechst-N$_3$ upon enzymatic incubation for 0–1800 s (purple: 0 min, dark blue: 30 s, blue: 60 s, green: 120 s, light green: 300 s, orange: 600 s, red: 1800 s) under hypoxic (A) or aerobic conditions (B). (C) Plot of fluorescence intensity of Hoechst-N$_3$ at 488 nm during enzymatic reaction. The data were obtained from Fig. 2A and B. (D and E) Emission of Cy-N$_3$ upon enzymatic incubation for 0–30 min (purple: 0 min, dark blue: 30 s, blue: 60 s, green: 120 s, light green: 300 s, orange: 600 s, red: 1800 s) under hypoxic (D) or aerobic conditions (E). (F) Plot of fluorescence intensity of Cy-N$_3$ at 718 nm during enzymatic reaction. The data were obtained from Fig. 2D and E.

Hoechst[21] with an azide group (Hoechst-N$_3$) as hypoxia indicator in the cell nucleus. We also prepared a fluorescent Cy5 derivative with the azide group (Cy-N$_3$) as a hypoxia indicator in mitochondria. Cy5 derivatives were known to accumulate in mitochondria because of their positive charge.[22] Both probes showed negligible fluorescence due to the quenching effect of azide group. However, they were reduced to fluorophores with primary amines once activated in cytosol of hypoxic cells, leading to bright fluorescence emission. After activation, the probes moved to their target organelles, cell nucleus and mitochondria, respectively. Both probes were not reversible and retained a distinct bright fluorescence once activated. Eventually, tracking and recording the history of changes in intracellular oxygen levels were possible with the proper use of each probe and observing the fluorescence emission in the cell nucleus and mitochondria.

Results and discussion

As shown in Scheme 1, we synthesized Hoechst-N$_3$ by azidation of Hoechst derivatives bearing amino group (Hoechst-NH$_2$).[23] On the other hand, Cy-N$_3$ was prepared according to a previously reported procedure.[24] Initially, we monitored the reactions of Hoechst-N$_3$ and Cy-N$_3$ in the presence of NADPH and rat liver microsome, which work as reducing agents. We measured the changes in their emission spectra in phosphate buffer solution (pH 7.4) during the enzymatic activation under hypoxic or aerobic conditions. Fig. 2 shows representative emission spectra of Hoechst-N$_3$ and Cy-N$_3$. Before activation by enzyme, these probes showed weak fluorescence (the quantum yield of fluorescence emission for Hoechst-N$_3$ and Cy-N$_3$ were estimated to be 0.13 and 0.01, respectively). Intense fluorescence of
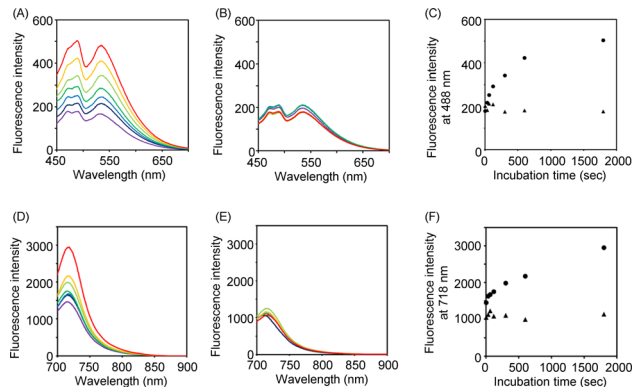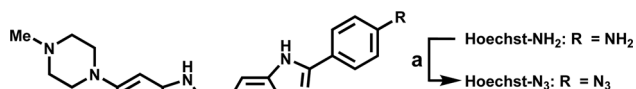

Scheme 1 Reagents and conditions: (a) NaNO$_2$, HCl, H$_2$O, then NaN$_3$, 94%.

Hoechst-N$_3$ was observed around 450–550 nm upon enzymatic activation under hypoxic conditions (0% O$_2$), whereas the activation at higher oxygen concentration (21% O$_2$) led to a lower fluorescence intensity. We also confirmed that enzymatic treatment of Hoecsht-N$_3$ under 10% O$_2$ conditions resulted in a negligible activation and lead to a weak fluorescence (Fig. S1†). Similar hypoxia-selective fluorescence was observed around 720 nm for Cy-N$_3$. These findings strongly indicate that Hoechst-N$_3$ and Cy-N$_3$ could be activated only in hypoxic cells.

We next applied Hoechst-N$_3$ and Cy-N$_3$ to live cell imaging of human lung adenocarcinoma cell line A549 to evaluate their specific accumulation and emission in target organelles. We employed A549 cells because several reductases are known to be activated in these cells selectively under hypoxic conditions.[25] The cells were incubated with Hoechst-N$_3$ or Cy-N$_3$ under hypoxic conditions and then subjected to confocal microscopy. As shown in Fig. 3, both fluorophores exhibited robust emission in the cells. Co-staining with RedDot or mitotracker revealed that Hoechst-N$_3$ accumulated in the nucleus, while that Cy-N$_3$ accumulated in mitochondria. The co-localization coefficients for Hoechst-N$_3$ to RedDot and Cy-N$_3$ to mitotracker were estimated to be 0.79 and 0.81, respectively. Additional experiments revealed that these probes showed negligible cytotoxicity toward A549 cells (Fig. S2†) and the minimum concentration of these probes required for biological imaging was 1 μM for both probes (Fig. S3†). Considering their behavior during the enzymatic activation, we applied them to cellular imaging of A549 cells that were cultured under hypoxic or aerobic conditions. As
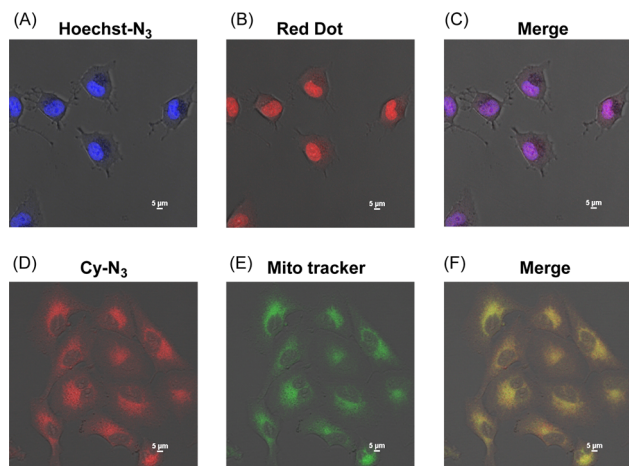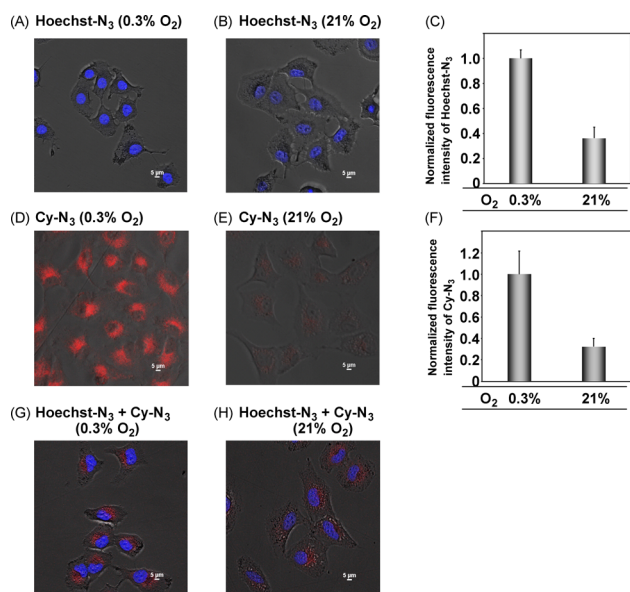
Fig. 3 Localization of Hoechst-N₃ (A–C) and Cy-N₃ (D–F) in A549 cells. The cells were incubated with Hoechst-N₃ (A) or Cy-N₃ (D) or and then cell nucleus (B) and mitochondria (E) were stained by organelle markers, RedDot and Mito tracker, respectively. (C and F) Merged pictures. Excitation wavelength was 405 and 640 nm for Hoechst-N₃ and Cy-N₃, respectively.


Fig. 4 Emission images of A549 cells as incubated with Cy-N₃ or Hoecsht-N₃. The cells were incubated with Hoechst-N₃ or Cy-N₃ under hypoxic (A, D and G: 0.3% O₂) or aerobic conditions (B, E and H: 21% O₂) and then, the images were immediately taken by means of confocal microscopy. Excitation wavelength was 405 and 640 nm for Hoechst-N₃ and Cy-N₃, respectively. The normalized fluorescence intensity obtained from the imaging experiments were described in Fig. C and F. (A–C) The cells were incubated with Hoechst-N₃ (5 μM) for 30 min. (D–F) The cells were incubated with Cy-N₃ (2.5 μM) for 4 h. (G and H) The cells were incubated with both Hoechst-N₃ (5 μM) and Cy-N₃ (1 μM) for 30 min.

shown in Fig. 4, administration of Hoechst-N₃ or Cy-N₃ allowed bright fluorescence at their target, cell nucleus or mitochondria in hypoxic cells. On the other hand, increasing oxygen concentration from 0.3% to 21% resulted in a weak emission.

Thus, the oxygen concentration-dependent emission of these fluorescent probes at their targets was observed. In separate experiments, we confirmed that the fluorescence emissions of reduction product of these probes were not affected by the oxygen concentration in the cells (Fig. S4†). We next conducted a simultaneous staining of mitochondria and nucleus in hypoxic cells using these probes. Both probes were administered to the hypoxic or aerobic cells, and then, the cells were subjected to microscopic evaluation (Fig. 4G and H). Although aerobic cells showed weak emission in cell nucleus and mitochondria, strong emission was observed in both target organelles in hypoxic cells. We also demonstrated similar cellular imaging of human colorectal cancer cell line HCT116 and human embryonic kidney (HEK)-293 cells using Hoechst-N₃ and Cy-N₃, and confirmed the hypoxia-selective emission in the cell nucleus and mitochondria after the administration of these probes (Fig. S5 and S6†).

We next attempted to identify the location of the enzymatic activation of these probes, Hoechst-N₃ and Cy-N₃, in the cells. For this purpose, Hoechst-N₃ and Cy-N₃ were administered to A549 cells, and then the cells were incubated for 30 min under aerobic conditions. After incubation, the medium was replaced with a fresh one, which was purged by nitrogen gas, and thus, cellular oxygen concentration was decreased. Microscopic evaluation revealed that the mitochondrial emission was enhanced, while nuclear emission intensity changed negligibly even after a decrease in intracellular oxygen levels (Fig. 5). These results strongly suggest that these probes were activated intracellularly and moved to their targets through the following processes; it seems that neither Hoechst-N₃ nor Cy-N₃ was activated in the cell nucleus, but that they were activated in cytosol. After activation of both probes in the cells, Hoechst-N₃ moved to cell nucleus promptly, while Cy-N₃ accumulated in mitochondria relatively slowly. Therefore, a decrease in oxygen levels led to an enhancement of mitochondrial emission, while negligible change in nuclear emission was observed even after the intracellular oxygen levels were decreased by a replacement of the medium having a low oxygen concentration. To
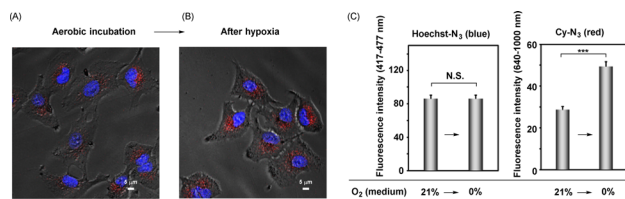
Fig. 5 (A and B) Fluorescence imaging of deoxygenation of A549 cells, which was induced by change of medium. The cells were loaded with Hoechst-N₃ (5 μM) and Cy-N₃ (1 μM), and then incubated for 30 min under aerobic conditions (21% O₂). Then, the medium was replaced by flesh medium which were kept under the 0% oxygen concentrations and the cells were further incubated under hypoxic conditions for 15 min. Before (A) and after (B) the replacement, the images were taken by means of microscopy. (C) Fluorescence intensity before and after stimulation. Fluorescence intensity of Hoechst-N₃ (left, 417–477 nm) and that of Cy-N₃ (right, 640–1000 nm) were obtained from Fig. 5A and B. ***$p < 0.001$ N. S.: not significant.

investigate further the location of Hoecst-N_3 and Cy-N_3 activation, cell deoxygenation using prominent mitochondrial uncouplers was assessed. The uncouplers increase the consumption of cellular molecular oxygen because they uncouple the respiratory chain and oxidative phosphorylation in the mitochondria to increase the rate of respiration. After incubation with both Hoecht-N_3 and Cy-N_3 for 30 min, the cells were stimulated by valinomycin as a mitochondrial uncoupler (Fig. S7†). A clear enhancement of emission was observed in mitochondria, but not in the cell nucleus. Thus, Hoecsht-N_3 rapidly moved to the nucleus and was largely unaffected by changes in oxygen concentration, whereas Cy-N_3 was strongly affected by deoxygenation and was reduced due to its slow transfer to the mitochondria.

The oxygen levels in solid tumor tissue were found to change significantly because of blood flow fluctuations.[26,27] Changes in oxygen concentration in the tissue impact therapeutic resistance, especially to radiotherapy,[4–6] and therefore, understanding the oxygen status in tumor cells is important for proper medical treatment. As mentioned above, Hoechst-N_3 and Cy-N_3 were activated in the hypoxic cells. Thus, we examined these probes to apply recording whether the cells were once hypoxic. As shown in Fig. 6A, we prepared four types of cells, A–A, A–H, H–A, and H–H cells, using these probes, and the cells were subjected to microscopy. First, the A–A cells were

prepared as follows. The A549 cells were incubated with Hoechst-N_3 for 15 min under aerobic conditions, and then, Cy-N_3 was administered. The resulting cells were further incubated under aerobic conditions for 30 min. The A–A cells were expected to show weak emission at both cell nucleus and mitochondria. Second, the A–H cells were prepared as follows. Initial incubation with Hoechst-N_3 under aerobic conditions for 15 min and following incubation with Cy-N_3 for 30 min under hypoxic conditions were conducted. The A–H cells were expected to show weak emission at cell nucleus, but the emission at mitochondria was expected to be bright. Third, for preparation of H–A cells, Hoechst-N_3 was administered to the cells, which were incubated for 15 min under hypoxic conditions. Then, Cy-N_3 was added and the cells were further incubated for 30 min under aerobic conditions. The H–A cells were expected to fluoresce at cell nucleus, while emission at mitochondria was expected to be weak. Finally, for preparation of H–H cells, hypoxic incubation of the cells in the presence of Hoechst-N_3 was conducted for 15 min, and then Cy-N_3 administration and further incubation under hypoxic conditions were implemented. Bright emission at both mitochondria and cell nucleus in H–H cells was expected. The images of these four types of cells were shown in Fig. 6B. As expected, the emission in the nucleus and mitochondria changed along with the change in oxygen concentration. Thus, determining the history of changes in the oxygen levels of living cells is possible based on the emission patterns of these molecular probes.

Conclusions

In summary, we prepared two types of hypoxia probes with azide groups as hypoxia-responsive units. These probes, Hoechst-N_3 and Cy-N_3, were reduced by intracellular enzymes, which selectively converted the azide group of these probes into primary amines under hypoxic conditions. Hoechst-N_3 was activated intracellularly under hypoxic conditions and then accumulated in the cell nucleus. On the other hand, Cy-N_3 accumulated at mitochondria after intracellular activation. Thus, they fluoresced at their targets in hypoxic cells. These probes could be used to record the oxygen status. When administered in the proper order, each probe was activated in response to cytoplasmic oxygen levels and accumulated in each target. In other words, by measuring the emission intensity of the cell nucleus and mitochondria, it was possible to estimate the history of oxygen concentration change in the cells. Thus, the probes designed in this study act as hypoxia indicator. The application of these probes to identification of oxygen status *in vivo* in progress.

Experimental section

Synthesis of Hoechst-N_3

Hoechst-NH_2 (18 mg, 4.25×10^{-5} mol) was dissolved in 6 M aq. HCl (200 μL), and $NaNO_2$ (14 mg, 2.0 mmol) in H_2O (1.0 mL) was added to the solution. The mixture was stirred at 0 °C for 30 min, and then, NaN_3 (14 mg, 2.2 mmol) in H_2O (1.0 mL) was added to the solution. The resulting solution was further stirred
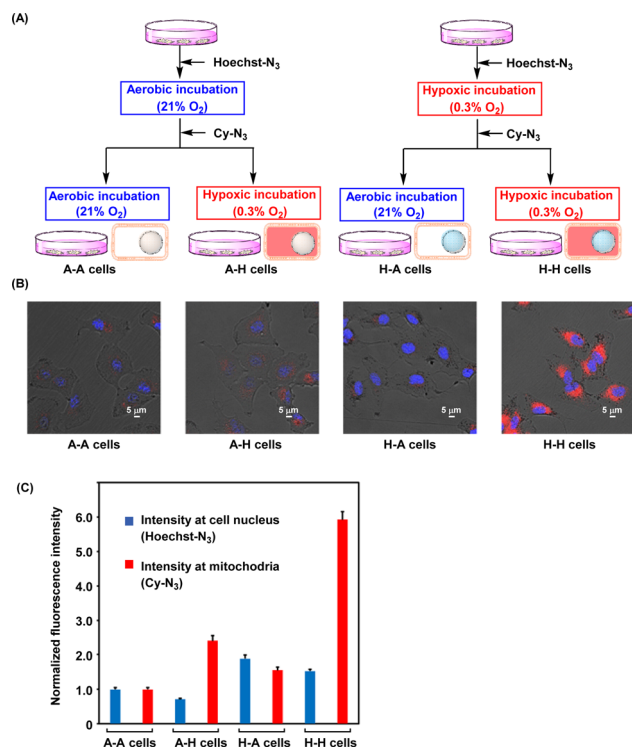
Fig. 6 (A) Schematic outline for recording oxygen variation in the cells on organelles. (B) Fluorescence imaging of A549 cells (A–A, A–H, H–A and H–H cells), which were treated in medium with different oxygen concentrations, according to the scheme shown in Fig. 6A. (C) Fluorescence intensity in the cells. Fluorescence intensity of Hoechst-N_3 (blue, 417–477 nm) and that of Cy-N_3 (right, 640–1000 nm) were obtained from Fig. 6B.

for 30 min at 0 °C and then, stirred for 30 min at ambient temperature. After the reaction, the resulting mixture was concentrated *in vacuo*. The crude product was purified by silica gel column chromatography ($CHCl_3$/MeOH/aq. NH_3 = 6/1/0.1) to give Hoechst-N_3 (18 mg, 94%) as red solid: MP > 300 °C; ^1H NMR (CD_3OD, 500 MHz) δ 8.08 (s, 1H), 7.94 (d, 2H, J = 8.5 Hz), 7.82 (dd, 1H, J = 1.0, 8.5 Hz), 7.71 (m, 1H), 7.43 (d, 1H, J = 5.5 Hz), 7.25 (m, 3H), 6.97 (dd, 1H, J = 2.0, 9.0 Hz), 3.18 (t, 4H, J = 4.5 Hz), 2.66 (t, 1H, J = 4.5 Hz), 2.37 (s, 3H); ^1H NMR (CD_3OD, 125 MHz) δ 154.6, 152.8, 152.0, 148.1, 142.2, 138.8, 132.2, 130.9, 128.5, 127.9, 125.6, 124.3, 121.2, 119.1, 118.2. 115.2, 114.9, 101.1, 54.8, 50.2, 44.6; FABMS (NBA) m/z 450 [(M + H)$^+$]; HRMS calcd for $C_{25}H_{24}N_9$ [(M + H)$^+$] 450.2155, found 450.2155.

Tracking enzymatic reduction of Hoechst-N_3 and Cy-N_3 using fluorescence spectroscopy

To establish a hypoxic condition, 500 nM of Hoechst-N_3 and Cy-N_3 in phosphate buffer (pH 7.4) were nitrogen purged. Then, rat liver microsome (1 μg mL^{-1}) and NADPH (1 μM) were added to these solutions and incubated at 37 °C. After the enzymatic reaction, Hoechst-N_3 solution was added to duplex DNA solution (500 nM) and further incubated for 1 h. These resulting mixtures were subjected to the measurement of fluorescence (excitation wavelengths were 405 nm for Hoechst-N_3 and 685 nm for Cy-N_3 respectively).

General procedure of fluorescence observation in living cells

A549 cells were cultured in DMEM containing 1% antibiotics and 10% FBS. The cells were seeded into 96-well plates (5000 cells per well) and cultured at 37 °C in a well-humidified incubator with 5% CO_2 and 95% air for 24 h. The cells were then incubated with aqueous solution of Hoechst-N_3 and Cy-N_3. After the incubation (30 min for Hoechst-N_3, 4 h for Cy-N_3), the medium was washed using Dulbecco's Phosphate Buffered Saline (DPBS) two times, and then the cells were observed using a confocal laser scanning microscope.

Imaging of alteration of hypoxic status using mitochondrial uncoupler stimuli

A549 cells were incubated with 5 μM of Hoechst-N_3 and 1 μM Cy-N_3 for 30 min under aerobic conditions. Then, 1 μM of valinomycin (1% DMSO) solution were added to the cells and additionally incubated for 2 h. The images of the cells before or after treatment with valinomycin was taken after wash of the cells by DPBS.

Recording of oxygen status of the cells

A459 cells were cultured at hypoxic (0.3%) and aerobic (21%) conditions for 24 h. After washing with DPBS, these cells were initially incubated with 5 μM of Hoechst-N_3 for 15 min and washed again with DPBS. Subsequently, 1 μM Cy-N_3 was added to the cells, and the resulting cells incubated further under hypoxic and aerobic conditions for 30 min. For an alternate change of cellular oxygen concentration, the medium with 0.3% O_2 conditions was replaced by the medium with 21% O_2

conditions. On the other hand, the cells with reduced oxygen levels were created by replacing the aerobic medium with a hypoxic medium. The medium for imaging hypoxic cells (0.3% O_2) was prepared by standing in the hypoxic chamber for 1 day. Finally, these cells were washed with DPBS and subjected to a confocal laser scanning microscopy.

Conflicts of interest

There are no conflicts to declare.

Acknowledgements

Notes and references

1 T. L. Place, F. E. Domann and A. J. Case, *Free Radical Biol. Med.*, 2017, **113**, 311–322.

2 M. Radisic, J. Malda, E. Epping, W. Geng, R. Langer and G. Vunjak-Novakovic, *Biotechnol. Bioeng.*, 2006, **93**, 332–343.

3 V. K. C. Ponnaluri, J. P. Maciejewski and M. Mukherji, *Biochem. Biophys. Res. Commun.*, 2013, **436**, 115–120.

4 A. Rakotomalala, A. Escande, A. Furlan, S. Meignan and E. Lartigau, *Front. Endocrinol.*, 2021, **12**, 742215.

5 B. Muz, P. de la Puente, F. Azab and A. K. Azab, *Hypoxia*, 2015, **3**, 83–92.

6 K. Begg and M. Tavassoli, *Cell Death Discovery*, 2020, **6**, 77.

7 K. G. Brurberg, M. Thuen, E.-B. M. Ruud and E. K. Rofstad, *Radiat. Res.*, 2006, **165**, 16–25.

8 D. M. Brizel, R. K. Dodge, R. W. Clough and M. W. Dewhirst, *Radiother. Oncol.*, 1999, **53**, 113–117.

9 M. W. Dewhirst, *Radiat. Res.*, 2009, **172**, 653–665.

10 N.-E. Choi, J.-Y. Lee, E.-C. Park, J.-H. Lee and J. Lee, *Molecules*, 2021, **26**, 217.

11 T. Yoshihara, S. Murayama, T. Masuda, T. Kikuchi, K. Yoshida, M. Hosaka and S. Tobita, *J. Photochem. Photobiol., A*, 2015, **299**, 172–182.

12 S. P.-Y. Li, T. S.-M. Tang, K. S.-M. Yiu and K. K.-W. Lo, *Chem.–Eur. J.*, 2012, **18**, 13342–13354.

13 B. Wang, Y. Liang, H. Dong, T. Tan, B. Zhan, J. Cheng, K. K.-W. Lo, Y. W. Lam and S. H. Cheng, *ChemBioChem*, 2012, **13**, 2729–2737.

14 V.-N. Nguyen and H. Li, *Molecules*, 2023, **15**, 6650.

15 D. Hara, Y. Umehara, A. Son, W. Asahi, S. Misu, R. Kurihara, T. Kondo and K. Tanabe, *ChemBioChem*, 2018, **19**, 956–962.

16 A. Son, A. Kawasaki, D. Hara, T. Ito and K. Tanabe, *Chem.–Eur. J.*, 2015, **21**, 2527–2536.

17 V. S. Hughes, J. M. Wiggins and D. W. Siemann, *Br. J. Radiol.*, 2019, **92**, 20170955.

18 J. Sun, Z. Liu, H. Yao, H. Zhang, M. Zheng, N. Shen, J. Cheng, Z. Tang and X. Chen, *Adv. Mater.*, 2023, **35**, 2207733.

19 L. J. O'Connor, I. N. Mistry, S. L. Collins, L. K. Folkes, G. Brown, S. J. Conway and E. M. Hammond, *ACS Cent. Sci.*, 2017, **3**, 20–30.

20 A. Herner, G. E. Girona, I. Nikić, M. Kállay, A. Edward, E. A. Lemke and P. Kele, *Bioconjugate Chem.*, 2014, **25**, 1370–1374.

21 A. Nakamura, K. Takigawa, Y. Kurishita, K. Kuwata, M. Ishida, Y. Shimoda, I. Hamachi and S. Tsukiji, *Chem. Commun.*, 2014, **50**, 6149–6152.

22 A. R. Nödling, E. M. Mills, X. Li, D. Cardella, E. J. Sayers, S.-H. Wu, A. T. Jones, L. Y. Luk and Y. H. Tsai, *Chem. Commun.*, 2020, **56**, 4672–4675.

23 K. Wiederholt, S. B. Rajur, J. Giuliano Jr, M. J. O'Donnell and L. W. McLaughlin, *J. Am. Chem. Soc.*, 1996, **118**, 7055–7062.

24 T. Ma, J. Zheng, T. Zhang and D. Xing, *Nanoscale*, 2018, **10**, 13462–13470.

25 W. A. Denny, *Pharmaceuticals*, 2022, **15**, 187.

26 R. D. Braun, J. L. Lanzen and M. W. Dewhirst, *Am. J. Physiol.*, 1999, **277**, H551–H568.

27 H. Yasui, S. Matsumoto, N. Devasahayam, J. P. Munasinghe, R. Choudhuri, K. Saito, S. Subramanian, J. B. Mitchell and M. C. Krishna, *Cancer Res.*, 2010, **70**, 6427–6436.